JACS
JOURNAL OF THE AMERICAN CHEMICAL SOCIETY

Subscriber access provided by American Chemical Society

Article

Guidelines in Implementing Enantioselective Indicator-Displacement Assays for α-Hydroxycarboxylates and Diols

Lei Zhu, Zhenlin Zhong, and Eric V. Anslyn

J. Am. Chem. Soc., **2005**, 127 (12), 4260-4269• DOI: 10.1021/ja0435945 • Publication Date (Web): 02 March 2005

Downloaded from http://pubs.acs.org on March 24, 2009

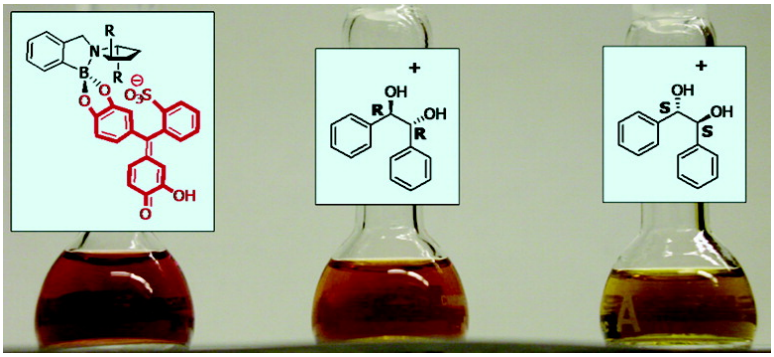

More About This Article

Additional resources and features associated with this article are available within the HTML version:

- Supporting Information
- Links to the 19 articles that cite this article, as of the time of this article download
- Access to high resolution figures
- Links to articles and content related to this article
- Copyright permission to reproduce figures and/or text from this article

View the Full Text HTML

ACS Publications
High quality. High impact.

Journal of the American Chemical Society is published by the American Chemical Society. 1155 Sixteenth Street N.W., Washington, DC 20036

J|A|C|S
ARTICLES
Published on Web 03/02/2005

Guidelines in Implementing Enantioselective Indicator-Displacement Assays for α-Hydroxycarboxylates and Diols

Lei Zhu, Zhenlin Zhong, and Eric V. Anslyn*

Contribution from the Department of Chemistry and Biochemistry, the University of Texas at Austin, Austin, Texas 78712

Received October 21, 2004; E-mail: anslyn@ccwf.cc.utexas.edu

Abstract: Enantioselective association events between boronic acid receptors and bifunctional substrates such as α-hydroxycarboxylates and vicinal diols were exploited to develop enantioselective indicator-displacement assays. It was found that the sensitivity of the assay could be tuned by using either colorimetric or fluorescent indicators. Mathematical principles were established for concurrent determination of concentration and enantiomeric excess (ee) of a chiral analyte, which has been a challenge to the high-throughput analysis of chiral samples. Furthermore, experimental protocols were optimized to maximize the chiral resolution of the assay and to improve the accuracy of the ee measurements.

Introduction

Competitive binding assays are established analytical methods in medicinal and clinical chemistry.[1] Currently, they are gaining substantial attention in more general chemical research areas.[2−4] A typical competitive binding assay constitutes a receptor and a signaling unit that also serves as a surrogate substrate. The signaling unit possesses an easily observable and quantifiable property, which is modulated in response to competitive binding with an analyte. For instance, modulation of absorbance or emission and the ability to catalyze a reaction[5−7] are common approaches. When the signaling unit is a pH or solvatochromic indicator, the assay is specifically called an indicator-displacement assay (Scheme 1).[8−10] The advantages of an indicator-displacement assay are as follows: (1) it eliminates the need to covalently incorporate the chromophore or fluorophore into the structures of receptors or analytes; (2) the indicators are exchangeable; (3) it has a detection mechanism that is not directly perturbed by the analyte structures; and (4) a secondary tuning of sensitivity and selectivity is available because of the participation of the indicator.[9,11,12] Rapid progress in the development of indicator-displacement assays has been made in recent years by our group[8,12−29] and others.[11,30−35] The usual molecular recognition driving forces are exploited in constructing successful indicator-displacement assays. So far, assays utilizing ion pairing, hydrogen bonding,[13,14] reversible covalent interactions,[22,28] metal coordination,[11,20,24,26,31,33−35] and combinations of these,[25,29] have been documented. Many physi-

Scheme 1. Indicator-Displacement and Enantioselective Indicator-Displacement Assays[a]

Indicator-Displacement Assay

$$H{:}I + G \rightleftharpoons H{:}G + I$$

$$\Delta Abs \text{ or } F/F_I = f([G]_t)$$

Enantioselective Indicator-Displacement Assay

$$H^*{:}I + G_R \rightleftharpoons H^*{:}G_R + I$$

$$H^*{:}I + G_S \rightleftharpoons H^*{:}G_S + I$$

$$\Delta Abs \text{ or } F/F_I = f([G]_t, ee)$$

[a] H, host/receptor; H*, chiral host/receptor; I, indicator; G, G_R, G_S, guest/analyte; ΔAbs, absorbance change; *F*, fluorescence intensity; F_I, fluorescence intensity of an unbound indicator, a constant; $[G]_t$, total guest concentration; ee, enantiomeric excess. In the enantioselective indicator-displacement assay, two enantiomers (G_R and G_S) in a chiral sample are competing for a fixed amount of receptor/indicator complex (H*:I).

(1) Perry, M. J. *Monoclonal Antibodies: Principles and Applications*; Wiley-Liss: New York, 1995; pp 107−120.
(2) Medintz, I. L.; Clapp, A. R.; Mattoussi, H.; Goldman, E. R.; Fisher, B.; Mauro, J. M. *Nat. Mater.* **2003**, *2*, 630−638.
(3) Höfner, G.; Wanner, K. T. *Angew. Chem., Int. Ed.* **2003**, *42*, 5235−5237.
(4) Qi, K.; Ma, Q.; Remsen, E. E.; Clark, C. G., Jr.; Wooley, K. L. *J. Am. Chem. Soc.* **2004**, *126*, 6599−6607.
(5) Wu, Q.; Anslyn, E. V. *J. Am. Chem. Soc.* **2004**, *126*, 14682−14683.
(6) Zhu, L.; Lynch, V. M.; Anslyn, E. V. *Tetrahedron* **2004**, *60*, 7267−7275.
(7) Hartig, J. S.; Grune, I.; Najafi-Shoushtari, S. H.; Famulok, M. *J. Am. Chem. Soc.* **2004**, *126*, 722−723.
(8) Wiskur, S. L.; Aït-Haddou, H.; Lavigne, J. J.; Anslyn, E. V. *Acc. Chem. Res.* **2001**, *34*, 963−972.
(9) Fabbrizzi, L.; Licchelli, M.; Taglietti, A. *J. Chem. Soc., Dalton Trans.* **2003**, 3471−3479.
(10) Connors, K. A. *Binding Constants, The Measurement of Molecular Complex Stability*; John Wiley and Sons: New York, 1987.
(11) Hortala, M. A.; Fabbrizzi, L.; Marcotte, N.; Stomeo, F.; Taglietti, A. *J. Am. Chem. Soc.* **2003**, *125*, 20−21.
(12) Piatek, A. M.; Bomble, Y. J.; Wiskur, S. L.; Anslyn, E. V. *J. Am. Chem. Soc.* **2004**, *126*, 6072−6077.
(13) Metzger, A.; Lynch, V. M.; Anslyn, E. V. *Angew. Chem., Int. Ed. Engl.* **1997**, *36*, 862−865.
(14) Metzger, A.; Anslyn, E. V. *Angew. Chem., Int. Ed.* **1998**, *37*, 649−652.
(15) Niikura, K.; Metzger, A.; Anslyn, E. V. *J. Am. Chem. Soc.* **1998**, *120*, 8533−8534.
(16) Niikura, K.; Bisson, A. P.; Anslyn, E. V. *J. Chem. Soc., Perkin Trans. 2* **1999**, 1111−1114.
(17) Cabell, L. A.; Monahan, M.-K.; Anslyn, E. V. *Tetrahedron Lett.* **1999**, *40*, 7753−7756.
(18) Lavigne, J. J.; Anslyn, E. V. *Angew. Chem., Int. Ed.* **1999**, *38*, 3666−3669.
(19) Wiskur, S. L.; Anslyn, E. V. *J. Am. Chem. Soc.* **2001**, *123*, 10109−10110.
(20) Aït-Haddou, H.; Wiskur, S. L.; Lynch, V. M.; Anslyn, E. V. *J. Am. Chem. Soc.* **2001**, *123*, 11296−11297.

10.1021/ja0435945 CCC: $30.25 **© 2005 American Chemical Society**

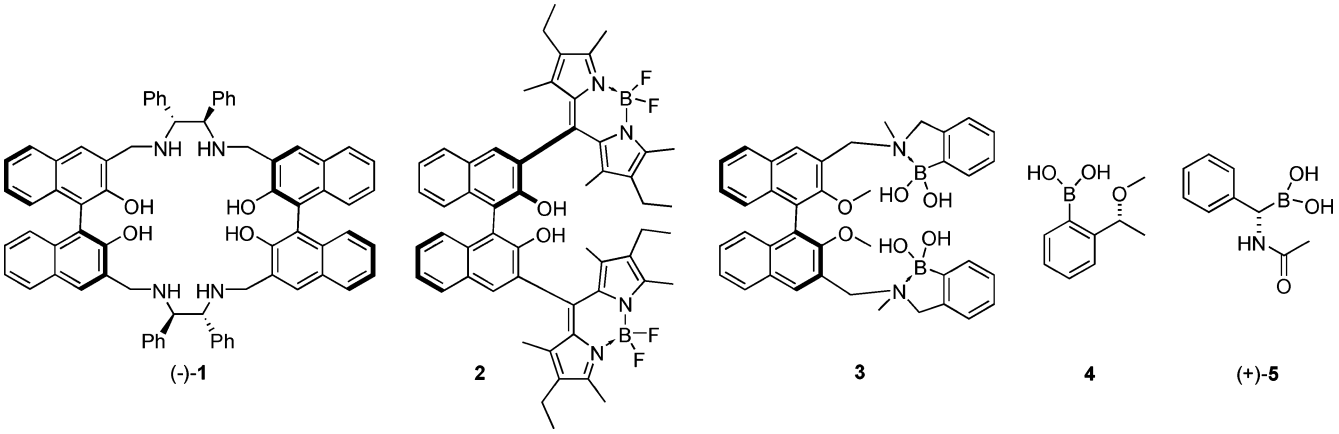

Figure 1. Examples of enantioselective chemosensors for various analytes through fluorescence spectroscopy (compounds (−)-**1**, **2**, and **3**) or ^{1}H NMR (**4** and **5**).

ologically and environmentally important targets, such as phosphate,[24,33] pyrophosphate,[34] citrate,[13] carbonate,[31] amino acids,[11] etc., can now be detected and quantified through indicator-displacement assays.

Despite the successes, the available applications of indicator-displacement assays have been limited to sensing the identity and quantity of given analytes. Determinations of other parameters of a sample, such as the enantiomeric excess (ee) of a chiral analyte,[36,37] are in growing demand. For example, high-throughput screening for potential enantioselective catalysts entails product-analyzing assays for rapid determination of both the yields and ee's from given catalytic reactions.[38] The double-parameter requirement increases the difficulty of assay design.[28,39−41] Traditional enantioselective optical chemosensors,[38,42,43] such as BINOL based compounds (−)-**1**[44] and **2**[45] in Figure 1, usually rely upon empirical ee calibration curves against absorbance or fluorescence intensity for each total concentration of the chiral analyte. The purpose of this study was to optimize indicator-displacement assays, using synthetically accessible receptors, to give simplified analytical protocols for rapid determination of concentrations and ee's of chiral samples.

It has been demonstrated that aromatic boronic acids interact strongly with bifunctional substrates such as sugars, diols, and α-hydroxycarboxylates in aqueous media.[46−48] A few boronic acid-based receptors show enantioselectivities. For example, a fluorescent sugar sensor (**3**) differentiates D- from L-monosaccharides.[49] Compounds **4**[50,51] and **5**[52] were developed to diastereomerically derivatize chiral diols, such that their ee's could be determined by ^{1}H NMR. Because boronic acid-based receptors have also been successfully incorporated into indicator-displacement assays for heparin[22] and scotch whiskey analysis,[19] we decided to base our initial studies of enantioselective indicator-displacement assays upon the reversible covalent interactions in aqueous media between aromatic boronic acids and α-hydrocarboxylates or vicinal diols.

In a preliminary study, an enantioselective indicator-displacement assay based on a chiral boronic acid receptor and a colorimetric indicator pyrocatechol violet (PV) was developed to determine the ee's of α-hydroxycarboxylate samples.[28] The concentration of a sample, which was needed for its ee determination, could be measured with an achiral displacement assay prior to the ee analysis. In a demonstration of the two-measurement protocol (Scheme 1), the ee values of three phenyllactic acid (PL) samples were determined with 15−20% error. In this paper, we report that the sensitivity of the assay can be tuned by changing the indicators, other substrates can be analyzed with this assay, and new experimental protocols are given that improve the accuracy of ee determination.

Results and Discussion

Design Criteria. In many reported boronic acid receptors (e.g., compound **3**), neighboring tertiary amino groups were

(21) McCleskey, S. C.; Metzger, A.; Simmons, C. S.; Anslyn, E. V. *Tetrahedron* **2002**, *58*, 621−628.
(22) Zhong, Z.; Anslyn, E. V. *J. Am. Chem. Soc.* **2002**, *124*, 9014−9015.
(23) McCleskey, S. C.; Griffin, M. J.; Schneider, S. E.; McDevitt, J. T.; Anslyn, E. V. *J. Am. Chem. Soc.* **2003**, *125*, 1114−1115.
(24) Tobey, S. L.; Anslyn, E. V. *Org. Lett.* **2003**, *5*, 2029−2031.
(25) Wiskur, S. L.; Floriano, P. N.; Anslyn, E. V.; McDevitt, J. T. *Angew. Chem., Int. Ed.* **2003**, *42*, 2070−2072.
(26) Zhong, Z.; Anslyn, E. V. *Angew. Chem., Int. Ed.* **2003**, *42*, 3005−3008.
(27) McCleskey, S. C.; Floriano, P. N.; Wiskur, S. L.; Anslyn, E. V.; McDevitt, J. T. *Tetrahedron* **2003**, *59*, 10089−10092.
(28) Zhu, L.; Anslyn, E. V. *J. Am. Chem. Soc.* **2004**, *126*, 3676−3677.
(29) Wiskur, S. L.; Lavigne, J. J.; Matzger, A.; Tobey, S. L.; Lynch, V. M.; Anslyn, E. V. *Chem.—Eur. J.* **2004**, *10*, 3792−3804.
(30) Gale, P. A.; Twyman, L. J.; Handlin, C. J.; Sessler, J. L. *Chem. Commun.* **1999**, 1851−1852.
(31) Fabbrizzi, L.; Leone, A.; Taglietti, A. *Angew. Chem., Int. Ed.* **2001**, *40*, 3066−3069.
(32) Stojanovic, M. N.; Landry, D. W. *J. Am. Chem. Soc.* **2002**, *124*, 9678−9679.
(33) Han, M. S.; Kim, D. H. *Angew. Chem., Int. Ed.* **2002**, *41*, 3809−3811.
(34) Fabbrizzi, L.; Marcotte, N.; Stomeo, F.; Taglietti, A. *Angew. Chem., Int. Ed.* **2002**, *41*, 3811−3814.
(35) Bioocchi, M.; Bonizzoni, M.; Fabbrizzi, L.; Piovani, G.; Taglietti, A. *Angew. Chem., Int. Ed.* **2004**, *43*, 3847−3852.
(36) Finn, M. G. *Chirality* **2002**, *14*, 534−540.
(37) Tsukamoto, M.; Kagan, H. B. *Adv. Synth. Catal.* **2002**, *344*, 453−463.
(38) Reetz, M. T. *Angew. Chem., Int. Ed.* **2001**, *40*, 284−310.
(39) Taran, F.; Gauchet, C.; Mohar, B.; Meunier, S.; Valleix, A.; Renard, P. Y.; Crèminon, C.; Grassi, J.; Wagner, A.; Mioskowski, C. *Angew. Chem., Int. Ed.* **2002**, *41*, 124−127.
(40) Chen, Y.; Shimizu, K. D. *Org. Lett.* **2002**, *4*, 2937−2940.
(41) Li, Z.; Bütikofer, L.; Witholt, B. *Angew. Chem., Int. Ed.* **2004**, *43*, 1698−1702.
(42) Pu, L. *Chem. Rev.* **2004**, *104*, 1687−1716.
(43) Zhao, J.; Fyle, T. M.; James, T. D. *Angew. Chem., Int. Ed.* **2004**, *43*, 3461−3464.
(44) Lin, J.; Zhang, H.-C.; Pu, L. *Org. Lett.* **2002**, *4*, 3297−3300.
(45) Beer, G.; Rurack, K.; Daub, J. *Chem. Commun.* **2001**, 1138−1139.
(46) Czarnik, A. W. *Acc. Chem. Res.* **1994**, *27*, 302−308.
(47) Wang, W.; Gao, X.; Wang, B. *Curr. Org. Chem.* **2002**, *6*, 1285−1317.
(48) Striegler, S. *Curr. Org. Chem.* **2003**, *7*, 81−102.
(49) James, T. D.; Sandanayake, K. R. A. S.; Shinkai, S. *Nature* **1995**, *374*, 345−347.
(50) Burgess, K.; Porte, A. M. *Angew. Chem., Int. Ed. Engl.* **1994**, *33*, 1182−1184.
(51) Resnick, S. M.; Torok, D. S.; Gibson, D. T. *J. Org. Chem.* **1995**, *60*, 3546−3549.
(52) Caselli, E.; Danieli, C.; Morandi, S.; Bonfiglio, B.; Forni, A.; Prati, F. *Org. Lett.* **2003**, *5*, 4863−4866.

Chart 1. Structures of Hosts/Receptors (H), Indicators (I), and Selected Guests/Analytes (G) in This Study[a]

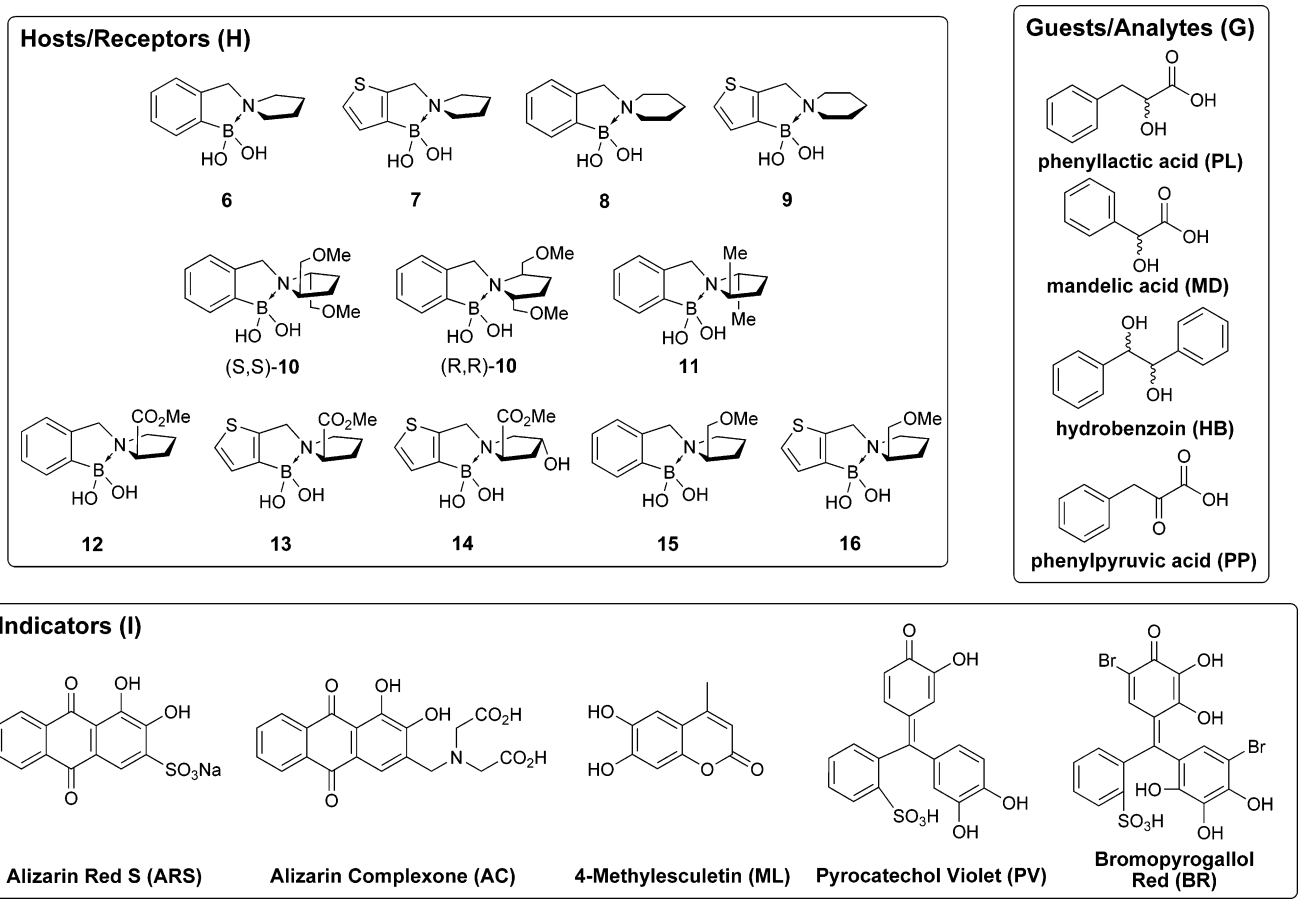

[a] Receptor structures are drawn with presumptive B−N bonds.

installed in proximity of boron atoms. Such amino groups were postulated to accelerate the association equilibria with their substrates, by serving as proton shufflers[53,54] or by modulating the thermodynamics of the association as Lewis bases for the boron atoms.[55] It was expected that the nitrogen atom coordinates with the electron-deficient boron atom to form a relatively rigid five-member-ring structure, as drawn for compound **3** in Figure 1.[55] However, there has been recent debate about the strength of the B−N interaction, and whether the bond remains intact in protic media.[56] Irrespective of this, we postulated that if stereogenic centers were installed in the vicinity of the postulated B−N bond in the receptor, the stereocenters would impart enantioselectivity to the association between the receptor and enantiomeric substrates. Hence, the chiral receptors **10**−**16** were devised and synthesized.

Synthesis. Boronic acid receptors **6**−**16** were prepared through reductive amination between *o*-formyl arylboronic acids and various pyrrolidine-based secondary amines (Scheme 2).[28] For the secondary amines without α-substituents, such as pyrrolidine or piperidine, the reductive amination was carried out smoothly with Schiff base formation in methanol followed by reduction with $NaBH_4$. When α-substituted secondary amines were used, the reduction was performed with $NaBH(OAc)_3$ to ensure a selective reduction of the iminium ions. The products were purified with alumina chromatography with satisfying yields (usually more than 70%).

Scheme 2. Synthesis of 2-Pyrrolidinylmethyl Phenylboronic Acids with Reductive Amination

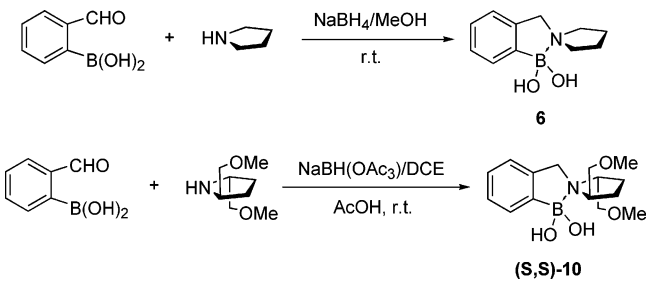

Enantioselective Fluorescent Indicator-Displacement Assay. Our preliminary account described the enantioselective associations between receptor (*S,S*)-**10** and various α-hydroxycarboxylates.[28] With PV serving as a colorimetric indicator (Figure 2), the assay was successfully applied in simultaneous determination of concentrations and ee's of unknown PL samples. In those measurements, the determined ee's had an average of 15% error from the actual values. The main objective of this study was to optimize the protocols to improve both the accuracy and sensitivity of the assay.

To devise assays with higher sensitivities and improved accuracy, fluorescent indicators were examined. The indicator 4-methylesculetin (ML, Figure 2) was found to undergo a large fluorescence intensity enhancement upon binding with bor-

(53) Wulff, G.; Lauer, M.; Bohnke, H. *Angew. Chem., Int. Ed. Engl.* **1984**, *23*, 741−742.
(54) Lauer, M.; Wulff, G. *J. Chem. Soc., Perkin Trans. 2* **1987**, 745−749.
(55) James, T. D.; Sandanayake, K. R. A. S.; Iguchi, R.; Shinkai, S. *J. Am. Chem. Soc.* **1995**, *117*, 8982−8987.
(56) Franzen, S.; Ni, W.; Wang, B. *J. Phys. Chem. B* **2003**, *107*, 12942−12948.

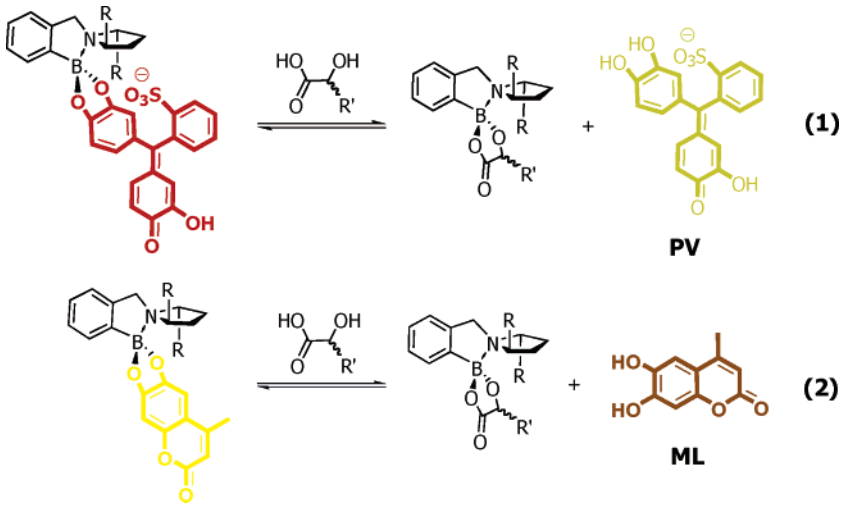

Figure 2. Enantioselective indicator-displacement assays for α-hydroxycarboxylates based upon (1) a colorimetric indicator (PV) and (2) a fluorescent indicator (ML).

onic acid receptors such as **8** and (*S*,*S*)-**10**. At pH 7.4 in a 75%/25% methanol/H_2O solution, the emission of ML was largely suppressed by the photoinduced electron transfer (PET) process from the hydroxyl groups to the coumarin moiety. Therefore, the free ML showed relatively weak fluorescence. Upon binding with boronic acid receptors, the electron deficient boron atoms raised the oxidation potential of the hydroxyl groups on ML, so that the presumptive PET process was thermodynamically disfavored.[57] Thus, when binding with compound **8**, the fluorescence from the coumarin moiety in the complex had at least a 10-fold enhancement over the free indicator (Figure 3A, B). Upon addition of PL, the fluorescence intensity decreased due to the competitive binding of PL to the receptors that released the indicator into solution (Figure 3C). The association constants between the receptors and ML were determined through the 1:1 binding isotherms (Figure 3B; see Supporting Information). The affinities of the receptors to PL were determined with a traditional competitive spectrophotometric method (Figure 3D).[10,22] The affinity data are listed in Table 1.

The fluorescence displacement profiles of PL with the achiral (**8**) and chiral ((*S*,*S*)-**10**) receptors are shown in Figure 4A. As expected, with chiral receptor (*S*,*S*)-**10**, the stronger associating PL enantiomer (L-PL) resulted in a more effective fluorescence quenching event than D-PL; while their fluorescence displacement profiles were virtually identical with achiral receptor **8**. The ee-dependent fluorescence quenching (of an indicator-receptor ensemble) profiles of PL at two different total substrate concentrations are displayed in Figure 4B. The profile derived from the larger total concentration of the guest (1.2 mM, blue) showed an overall more effective fluorescence quenching with an otherwise similar shape. The fluorescence intensities were growing with the increasing ee of the weaker associating enantiomer, D-PL. The slope of the emission intensity as a function of ee (dF/dee) was greater when the ee of D-PL became larger (Figure 4B), because the concentration change of the stronger associating enantiomer (Δ[L-PL]) had a more pronounced effect in modulating fluorescence intensity when its concentration ([L-PL]) was relatively small than vice versa.[28] Through this study, an enantioselective indicator-displacement assay for PL was established based upon enantioselective associations between receptor (*S*,*S*)-**10** and D/L-PL and the utilization of the fluorescent indicator ML.

Mathematical Analysis of Solution Equilibria. Because the enantioselective fluorescent indicator-displacement assay follows solution equilibria (Scheme 1),[28] a relationship between the ee of a sample and the fluorescence intensity can be established. One of our goals was to discover if iterative curve fitting of the F/F_I vs ee curve would give a more accurate ee assay than previously reported.[28]

The fluorescence intensity F is related to both the free and bound indicator I and HI via eq 1

$$F = k_I b[\mathrm{I}] + k_{HI} b[\mathrm{HI}] \qquad (k \equiv 2.3 I_0 \phi \epsilon) \tag{1}$$

(I_0, the intensity of the excitation source; ϕ, fluorescence quantum yield; ϵ, molar absorptivity at the excitation wavelength; b, path length).[58] With F_I defined as the fluorescence intensity from the free indicator ($F_I \equiv k_I b[\mathrm{I}]_t$), eq 1 is converted to eq 2

$$F/F_I = [\mathrm{I}]/[\mathrm{I}]_t + n[\mathrm{HI}]/[\mathrm{I}]_t \qquad (n \equiv k_{HI}/k_I,\ F_I \equiv k_I b[\mathrm{I}]_t) \tag{2}$$

When a mixture of enantiomeric guests is present, the concentrations of all the solution species are defined by three solution equilibria eqs 3−5

$$[\mathrm{HI}] = K_I[\mathrm{I}][\mathrm{H}] \tag{3}$$

$$[\mathrm{HG_R}] = K_R[\mathrm{G_R}][\mathrm{H}] \tag{4}$$

$$[\mathrm{HG_S}] = K_S[\mathrm{G_S}][\mathrm{H}] \tag{5}$$

Other restricting factors include mass balances for the receptor

(57) de Silva, A. P.; Gunaratne, H. Q. N.; Gunnlaugsson, T.; Huxley, A. J. M.; McCoy, C. P.; Rademacher, J. T.; Rice, T. E. *Chem. Rev.* **1997**, *97*, 1515−1566.

(58) Lakowicz, J. R. *Principles of Fluorescence Spectroscopy*; Plenum Press: New York, 1999.

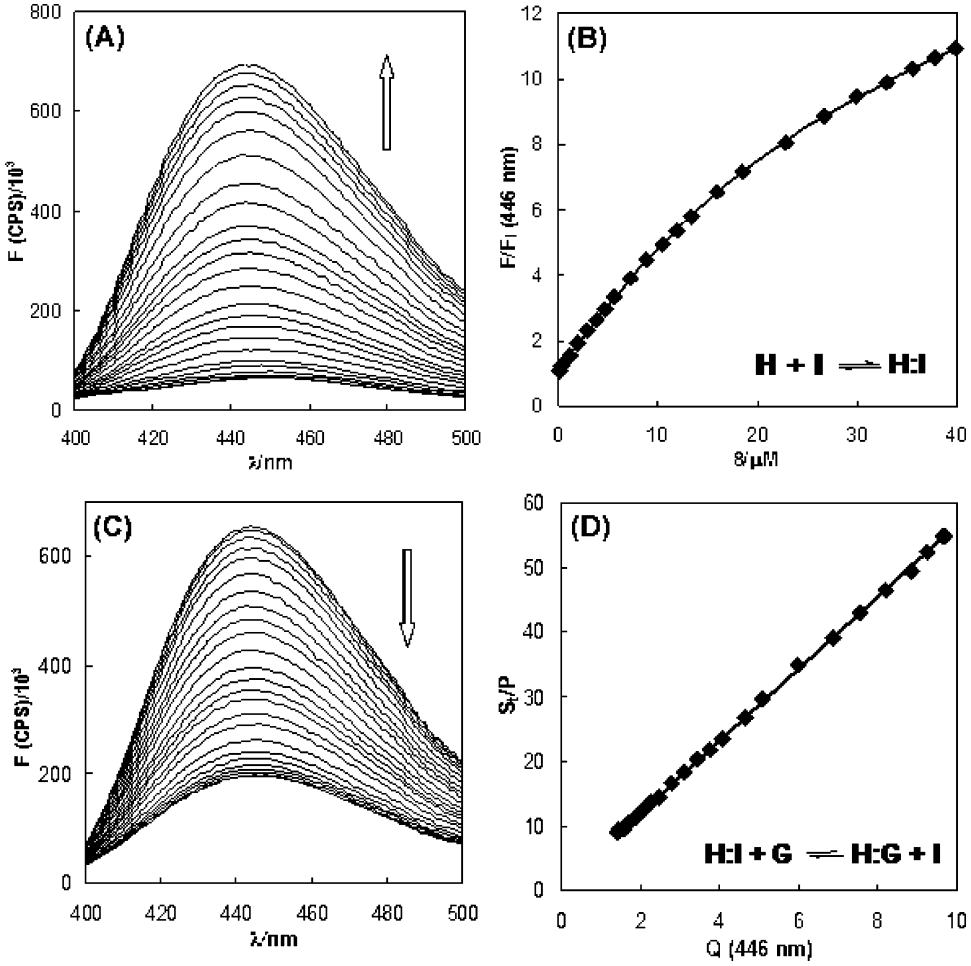

Figure 3. (A) Fluorescence spectra of ML (3.6 μM) in 75% methanolic aqueous solution buffered with 10 mM HEPES at pH 7.4 (default buffer) in the presence of 0−40 μM **8**. Fluorescence intensity (F) is shown as counts per second (CPS). (B) Curve fitting of relative fluorescence intensity vs receptor (**8**) concentration at 446 nm (excited at 362 nm), F_I (fluorescence intensity of the unbound indicator ML). (C) Fluorescence spectra of ML (3.6 μM) and **8** (31.9 μM) in the default buffer in the presence of 0−1.5 mM of L-PL. (D) S_t/P vs Q plot from the competitive fluorimetric method, derived from the competitive spectrophotometric method,[10] with data taken at 446 nm.

Table 1. Association Constants (K/10^3 M^{-1}) of Boronic Receptors (**8**, (*S*,*S*)-**10**) with Indicator ML and D/L-PL[a]

	ML	D-PL	L-PL
8	24.92 ± 0.07	4.50 ± 0.09 (4.38 ± 0.05)	4.56 ± 0.08 (4.39 ± 0.06)
(*S*,*S*)-**10**	30.19 ± 1.55	4.35 ± 0.07 (4.27 ± 0.24)	10.86 ± 0.03 (10.45 ± 0.10)

[a] Measured via 1:1 binding isotherms or a competitive fluorimetric method in the default buffer (Figure 3, footnote). Association constants obtained from iterative curve fitting are shown in the parentheses for comparison.

(H), the indicator (I), and the analyte (G_R, G_S), as well as the definition of ee (eqs 6−9)

$$[H] + [HI] + [HG_R] + [HG_S] = [H]_t \quad (6)$$

$$[I] + [HI] = [I]_t \quad (7)$$

$$[G_R] + [G_S] + [HG_R] + [HG_S] = [G]_t \quad (8)$$

$$ee_R = \frac{([G_R] + [HG_R]) - ([G_S] + [HG_S])}{[G]_t} \quad (9)$$

By rearranging the equations with the aid of the commercial software Mathematica,[59] the concentrations of all the solution species ([I], [HI], [HG_R], [G_R], [HG_S], [G_S], and [H]) can be expressed as functions of measurable parameters ([H]$_t$, [I]$_t$, [G]$_t$, K_I, K_R, K_S, and n). When these symbolic expressions are introduced into eq 6, an implicit F/F_I vs ee relationship is given in eq 10.

$$\frac{(F/F_I - 1)[I]_t}{n - 1} + \frac{(F/F_I - 1)}{K_I(n - F/F_I)} + \frac{K_R[G]_t(1 + ee_R)(1 - F/F_I)}{2[(F/F_I)(K_I - K_R) - (nK_I - K_R)]} + \frac{K_S[G]_t(1 - ee_R)(1 - F/F_I)}{2[(F/F_I)(K_I - K_S) - (nK_I - K_S)]} = [H]_t \quad (10)$$

Other parameters can be independently determined through 1:1 binding isotherms (K_I, n), competitive binding methods (K_R, K_S), gravimetric measurements ([H]$_t$, [I]$_t$), and achiral indicator-displacement assays ([G]$_t$), respectively. If K_R equals K_S, as in a displacement assay with an achiral host, eq 10 can be rearranged to give the typical equation for the competitive spectrophotometric method (see Supporting Information).[10] The cor-

(59) http://www.wolfram.com.

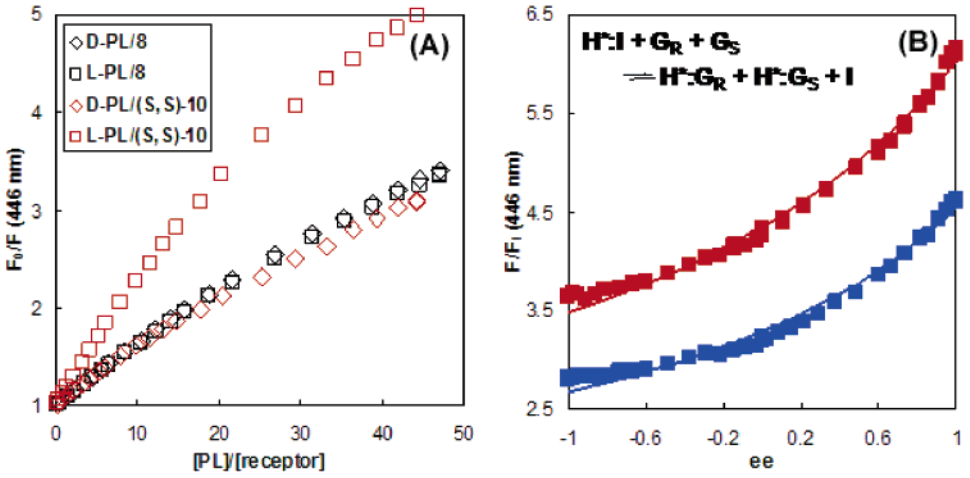

Figure 4. (A) Fluorescence quenching profiles at 446 nm of ML (3.6 μM) and receptors (*S*,*S*)-**10** (34 μM) or **8** (31.9 μM) in the default buffer (footnote, Figure 3) with increasing concentration of D- or L-PL, displayed in a Stern−Volmer format. Data are shown as the averages of two measurements. F, fluorescence intensity (CPS); F_0, fluorescence intensity (CPS) at the inception. (B) Relative fluorescence intensity change at 446 nm of ML (3.6 μM), receptor (S,S)-**10** (34 μM), and analyte solutions upon increasing ee of D-PL. F_I, fluorescence intensity (CPS) of the free indicator at the designated concentration (see the next section); red, $[G]_t = 676$ μM; blue, $[G]_t = 1.2$ mM. The solid lines are theoretical curves resulted from iterative data fitting. The association constants extracted from the fitting are (averages from two total concentrations): $K_R = (3.39 \pm 0.03) \times 10^3$ M^{-1}; $K_S = (9.79 \pm 0.48) \times 10^3$ M^{-1} (see the next section).

relation between the traditional approach and our analysis provides validation for the F/F_I vs ee relationship shown in eq 10.

When all the measurable parameters (K_I, n, K_R, K_S, $[H]_t$, $[I]_t$, $[G]_t$) were introduced into eq 10, calibrating curves of F/F_I vs ee with given $[G]_t$ concentrations were generated. Although the calculations were very close, they did not always sufficiently reproduce the experimental data for a good ee determination (see Supporting Information). This is largely due to the fact that the parameters are necessarily determined under somewhat different conditions. Fluctuations in room temperature, the power supply of the fluorimeter, and the sensitivity of the detection system, etc., over the time when the measurements of the parameters were conducted contributed to the discrepancy between the calculated and experimental F/F_I vs ee data. Therefore, we wished to develop a method enabling iterative data fitting of experimental F/F_I vs ee curves by adjusting K_R and K_S, with secondary consideration of other parameters.[60] Curve fitting of the fourth-order polynomial $F/F_I = f(\text{ee})$ relationship (eq 10) presented a daunting task. Even traditional competitive binding curves without the ee consideration had not been previously fit *iteratively*.[12] However, we decided that the direct determination of binding constants from competitive binding curves through iterative data fitting would be feasible with the use of commercial software.

As a start, the nonlinear function $A = f([G]_t)$ in Scheme 1 was studied without the *ee* consideration. The absorbance was correlated to indicator concentrations through Beer's Law (eq 11)

$$\text{Beer's Law: } A = \epsilon_I b[I] + \epsilon_{HI} b[HI] \quad (11)$$

The [I] and [HI] values were dictated by solution equilibria among H, I, and G (eqs 12 and 13),

$$\text{Solution equilibria: } [HI] = K_I[I][H] \quad (12)$$

$$[HG] = K_G[G][H] \quad (13)$$

with restrictions from their mass totals (eqs 14−16)

$$\text{Mass balance: } [I] + [HI] = [I]_t \quad (14)$$

$$[H] + [HI] + [HG] = [H]_t \quad (15)$$

$$[G] + [HG] = [G]_t \quad (16)$$

By rearranging eqs 12 and 14, [I] and [HI] were expressed as functions of [H], and subsequently these functions were introduced into the Beer's Law eq 11 to afford eq 17

$$\text{Beer's Law: } A = \epsilon_I b[I]_t/(1 + K_I[H]) + \epsilon_{HI} b K_I[H][I]_t/(1 + K_I[H]) \quad (17)$$

in the form of $A = f([H])$. Similarly, [HG] was expressed as a function of [H] by rearranging eqs 13 and 16. The symbolic values of [HI] and [HG] in terms of [H] were introduced into the mass balance of $[H]_t$ (eq 15) to afford a cubic equation in [H] (eq 18)

$$K_I K_G[H]^3 + (K_I + K_G + K_I K_G[I]_t + K_I K_G[G]_t - K_I K_G[H]_t)[H]^2 + (1 + K_I[I]_t + K_G[G]_t - K_I[H]_t - K_G[H]_t)[H] - [H]_t = 0 \quad (18)$$

At this point, all the parameters in eqs 17 and 18, except for K_G that was to be determined, were known from gravimetric means ($[H]_t$, $[I]_t$, $[G]_t$) or previous measurements (ϵ_I, ϵ_{HI}, K_I).

Actual curve fitting was achieved by the nonlinear least squares curve fitting module of the commercial software Origin that ran a brief user-defined function compiled with the LabTalk computation language integrated in the software package. The compiled function had a two-step iterative cycle. First, an arbitrarily estimated value was assigned to K_G. [H] was subsequently obtained from solving the cubic eq 18 based on

(60) Unlike other parameters, the determination of K_R and K_S through competitive binding methods always depends on the values of other constants, such as K_I, ϵ_I, and ϵ_{HI}. Therefore, K_R and K_S would not be as accurate as the other parameters. Hence, they are considered more adjustable than other parameters.

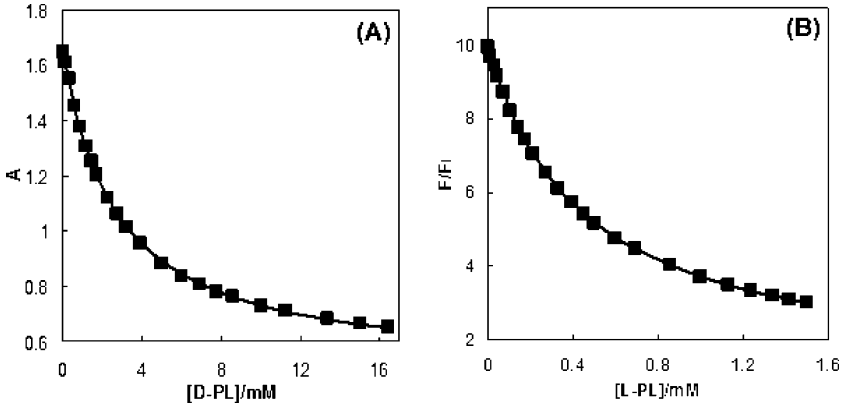

Figure 5. (A) (■) Absorbance at 520 nm of PV (149 μM) and receptor (*S*,*S*)-**10** (0.51 mM) in the default buffer (Figure 3, footnote) with increasing concentration of D-PL; solid line, theoretical curve from iterative fitting in Origin with a user defined function. (B) (■) Fluorescence intensity (F/F_I) of ML (3.6 μM) and receptor **8** (31.9 μM) in the default buffer with increasing concentration of L-PL; solid line, theoretical curve from iterative fitting in Origin with a user defined function.

the Newton−Raphson method.[61] Because of the multiplicity of the roots from a cubic equation, it should be stressed that a judicious choice of the initial value of [H] ($[H]_{ini}$ for the Newton−Raphson method) is pivotal to the success of obtaining a reasonable calculated value of [H]. Second, the obtained [H] was introduced to eq 17 to afford a calculated absorbance (*A*) value. This value was compared with the measured *A* value by the curve-fitting module to evaluate the quality of the initially assigned K_G. The program then generated a new, and usually superior, value for K_G based upon the Levenberg−Marquardt algorithm (see Origin manual), and the above process was repeated until the best value of K_G was found.

The above algorithm can be applied generally in cases involving two interdependent equilibria. For our indicator-displacement studies, there are usually six parameters besides the variables *A* and $[G]_t$, K_G, K_I, $[H]_t$, $[I]_t$, ϵ_I, and ϵ_{HI}, that can be adjusted to obtain a satisfying curve fitting (i.e. $R^2 > 0.99$). The following procedure was established to restrict the variations of the parameters in order to afford a reasonable and reproducible K_G. $[H]_t$, $[I]_t$, which were obtained gravimetrically, and K_I, which was independently determined from a 1:1 binding isotherm, were treated as fixed parameters. The extinction coefficients ϵ_I and ϵ_{HI} were dependent on experimental conditions (temperature, background absorption, etc.). Therefore, they were allowed for variation. Various data sets were then fit successfully with this method, with one example shown in Figure 5A. Selected results are shown in parallel with association constants determined by the traditional competitive spectrophotometric method in Table 5. A similar approach was applied to data sets based on fluorescence measurements (one example in Figure 5B), and the results are shown in Table 1. The fitting quality exemplified in Figure 5, the accuracy displayed in Tables 1 and 5, the generality to multiple equilibria problems, and the ease of operation make this approach our method of choice.

Next, the algorithm targeting iterative curve fitting of an *A* or $F/F_I = f(\text{ee})$ calibration curve in an enantioselective indicator-displacement assay was developed in a similar manner, but with one step of higher complexity (see Supporting Information). In an assay based upon fluorescence, there were seven parameters besides variables F/F_I and ee: K_I, *n*, K_R, K_S, $[I]_t$, $[H]_t$, and $[G]_t$ (eq 10). Gravimetric values ($[I]_t$, $[H]_t$, $[G]_t$), K_I, and *n* from a 1:1 binding isotherm were treated as invariable. Now the data were fit (Figure 4B) by varying the values of the association constants between the chiral receptor and the enantiomers of the analyte (K_R, K_S). As a validation to this approach, the association constant values obtained from the fitting of the ee curves (see captions for Figures 4B and 6D) matched very well (the errors were less than 5% as shown in Table 1) to the values determined from both the traditional competitive binding method and the iterative fitting of competitive binding curves with enantiomerically pure substrates (Tables 1 and 5).

Table 2. Determination of ee's of 10 PL Samples by Fluorimetry

sample no.	1	2	3	4	5
actual ee ($[G]_t = 676\ \mu M$)	0.90	0.33	0	−0.67	−1.00
determined ee	0.92	0.26	−0.13	−0.72	−0.89
actual ee ($[G]_t = 1.2$ mM)	0.98	0.21	−0.03	−0.38	−0.98
determined ee	1.02	0.18	−0.09	−0.26	−0.57

ee Determination of Unknown PL Samples via Fluorimetry. We set forth to use the K_R and K_S obtained from the iterative fitting of F/F_I vs ee curves for determination of ee's of unknown PL samples by solving eq 10. We found that the association constants obtained by iteration gave more accurate results than those extracted from competitive binding curves with enantiomerically pure PLs. This is because some of the factors affecting the accuracy of the K_R and K_S values, such as the variation of ionic strength and subtle volume changes during the measurements, are kept to a minimum in the F/F_I vs ee measurements. As more and more F/F_I vs ee data at different concentrations are accumulated, the average values of K_R and K_S obtained with different total analyte concentrations will move closer to their true values.

From the available F/F_I vs ee data (Figure 4B), 10 data points (5 for each concentration) were randomly selected and designated as samples with unknown ee's. The curves were fit with the remaining data points to obtain two sets of K_R and K_S values. The average K_R (3394 M^{-1}) and K_S (9791 M^{-1}) were used in conjunction with other parameters ($K_I = 31744\ M^{-1}$, $[I]_t = 3.6 \times 10^{-6}\ M^{-1}$, $[H]_t = 34 \times 10^{-6}\ M^{-1}$, $[G]_t = 676 \times 10^{-6}\ M^{-1}$ or $1.2 \times 10^{-3}\ M^{-1}$, and $n = 21.3$) in eq 10 to calculate the ee's of the unknown samples based on their fluorescence intensity. The determined ee values were in good agreement with the actual numbers (Table 2).[62] By using fluorimetry and

(61) Acton, F. S. *Numerical Methods That Work*; Harper & Row: New York, 1970.

Table 3. Association Constants ($K_I/10^3$ M^{-1}) of Receptor **6** with Various Indicators and Their Bathochromic or Hypsochromic Responses upon Association

indicator	ARS	AC	ML	PV	BR
batho-/hypsochromic shift/nm	540 → 456	525 → 440	294 → 364	440 → 480	565 → 470
$K_I/10^3$ M^{-1}	50	13[a]	8.7	2.3[a]	8.1

[a] Data reported in a previous Communication.[28]

Table 4. Association Constants ($K_I/10^3$ M^{-1}) of Boronic Receptors (**6**−**16**) with Indicator AC[a,b]

host	**6**	**7**	**8**	**9**	(*S*,*S*)-**10**	(*R*,*R*)-**10**	**11**	**12**	**13**	**14**	**15**	**16**
$K_I/10^3$ M^{-1}	13[b]	16	48	22	63[b]	61[b]	53	−	*1.8*	*0.94*	57[b]	21

[a] Receptors **12**−**14** do not associate with AC. Their affinities to indicator ARS are shown in *italics* instead. [b] Data reported in a previous Communication.[28]

Table 5. Association Constants ($K_G/10^3$ M^{-1}) of Selected Receptors with Selected Substrates (Determined via Competitive Spectrophotometric Method) and Indicator PV[b]

	PV	D-PL	L-PL	*R*-MD	*S*-MD	(*R*,*R*)-HB	(*S*,*S*)-HB
6	2.3[a]	1.3[a](1.3)	1.3[a](1.3)	0.64	0.71	0.54 (0.53)	0.53 (0.50)
7	3.0	1.6	1.6	0.90	0.93	0.42 (0.48)	0.42 (0.40)
(*S*,*S*)-**10**	13[a]	3.4[a](2.9)	9.6[a](8.4)	2.4[a]	3.0[a]	0.49 (0.46)	1.3 (1.3)
11	12	3.1	4.6	2.1	3.2	N.D.[c]	N.D.

[a] Data reported in a previous Communication.[28] [b] Selective association constants obtained from direct iterative curve fitting are shown in the parentheses for comparison. [c] N.D.: not determined.

K_R and K_S values determined from the F/F_I vs ee curves, the average error was found to be 7%.

Displacement with Other Substrates. A secondary goal of the study reported herein was to extend the analyte range of our technique. Therefore, the affinities among different receptors, indicators, and guest molecules other than PL were determined via an absorption spectroscopic method. Among all the indicators studied, alizarin red S (ARS)[63] has the largest affinity for the receptors. Generally, the affinities of indicators to a given receptor follow the sequence ARS > AC > ML ≈ BR > PV (Table 3). The visible absorption maxima of ARS, AC, and PV undergo dramatic shifts upon binding with the receptors (Table 3), which establish them as effective colorimetric indicators. BR also undergoes a large absorption maxima shift when associating with the receptors. However, the extinction coefficient of its bound form (ϵ_{HI}) is too small to enable an actual color change. ML absorbs in the UV region, and its application as a fluorescent indicator was described in the previous section. In terms of receptors, except for the proline-derived compounds (**12**−**14**) which have no measurable associations to any indicators except ARS, all the others have comparable affinities to the indicators (Table 4).

The association properties of receptors **6**, **7**, (*S*,*S*)-**10**, and **11** with selective substrates were studied with indicator-displacement assays. PV was selected as the indicator, and the association constants are listed in Table 5. Achiral receptors **6** and **7** showed no selectivity between enantiomers of the guest molecules as required by first principles of stereochemistry. The receptors had stronger affinities toward α-hydroxycarboxylates (e.g., PL and mandelic acid (MD)) than the vicinal diol hydrobenzoin (HB), which is consistent with other results.[29,64] Chiral receptor (*S*,*S*)-**10**, and compound **11** to a lesser extent, displayed enantioselectivities toward both α-hydroxycarboxylates and the diol HB. Another diol studied, 3,4-butanediol, showed no measurable affinity to **8**. Other bifunctional substrates that were investigated include *β*-hydroxyacid (3-hydroxybutyric acid), amino acids (*tert*-leucine), BINOL, amino alcohol (phenylglycinol), and ascorbic acid. Ascorbic acid showed considerable affinity via a very slow equilibrium (the color change occurs during a course of several hours). All other substrates studied do not appear to associate with the boronic receptors.

To employ the enantioselective binding of (*S*,*S*)-**10** in a sensing application, a protocol was needed to maximize the sensitivity of the assay to the ee variations of chiral samples. This included the selection of an indicator, a proper concentration for the indicator, and an optimized indicator/receptor ratio. Fabbrizzi et al. showed from extensive studies that it is ideal to have an indicator with an affinity between that of two competing analytes ($K_G \gg K_I \gg K_{G'}$),[9] which are two enantiomers in our current study. However, this condition cannot always be easily met. For example, in our study, the analytes' affinities to the receptors were generally weaker than that of the indicators (Tables 3, 5). Therefore, the indicator PV was chosen because its affinity to the receptor was the closest to the analytes among all the candidates. In this case, the equilibrium H + I ⇌ H:I was most sensitive to the competition of the enantiomeric analytes G_R and G_S.

Next, for selecting a proper concentration of the indicator, the chiral resolution of an enantioselective indicator-displacement assay at a given analyte concentration and a given wavelength was defined as the absorbance difference between the enantiomers ($\Delta A = |A_R - A_S|$) for the ease of the analysis. ΔA, the chiral resolution, is a function of K_R, K_S, K_I, $[H]_t$, $[I]_t$, etc., as discussed in the last section. A set of empirical principles was applied for maximizing the assay's chiral resolution (ΔA). When $K_R = K_S$ and $\Delta A = 0$, the assay loses its enantioselectivity. Consequently, the primary factor determining the enantioselective response of the assay should be the enantioselectivity of the receptor to the enantiomers of the analyte. The secondary factor is the signal amplifying power (ϵ or ϕ) of the indicator, which is proportional to ΔA (or ΔF in a fluorescent assay). Therefore, the indicator concentration should be as high as possible within the constraint of Beer's Law in order to maximize ΔA.

Finally, it is obvious that the assay's enantioselecting power should increase with increasing concentration of the chiral receptor ($\Delta A \propto [H]_t$). On the other hand, if the indicator is saturated by an excess amount of the receptor, there will be a delayed overall response to the analyte, because the analyte will first interact directly with the free receptor molecules rather than participating in the displacement event.[12] As a result, the overall sensitivity of the assay will be reduced. Through extensive optimization, it was observed that an $[H]_t/[I]_t$ ratio which gives

(62) Except for the first datum when $[G]_t = 1.2$ mM. Such impaired accuracy is due to the reduced sensitivity at the stronger binding enantiomer end of F/F_I vs ee curves, as discussed previously.

(63) Springsteen, G.; Wang, B. *Chem. Commun.* **2001**, 1608−1609.
(64) Gray, J.; C. W.; Houston, T. A. *J. Org. Chem.* **2002**, *67*, 5426−5428.

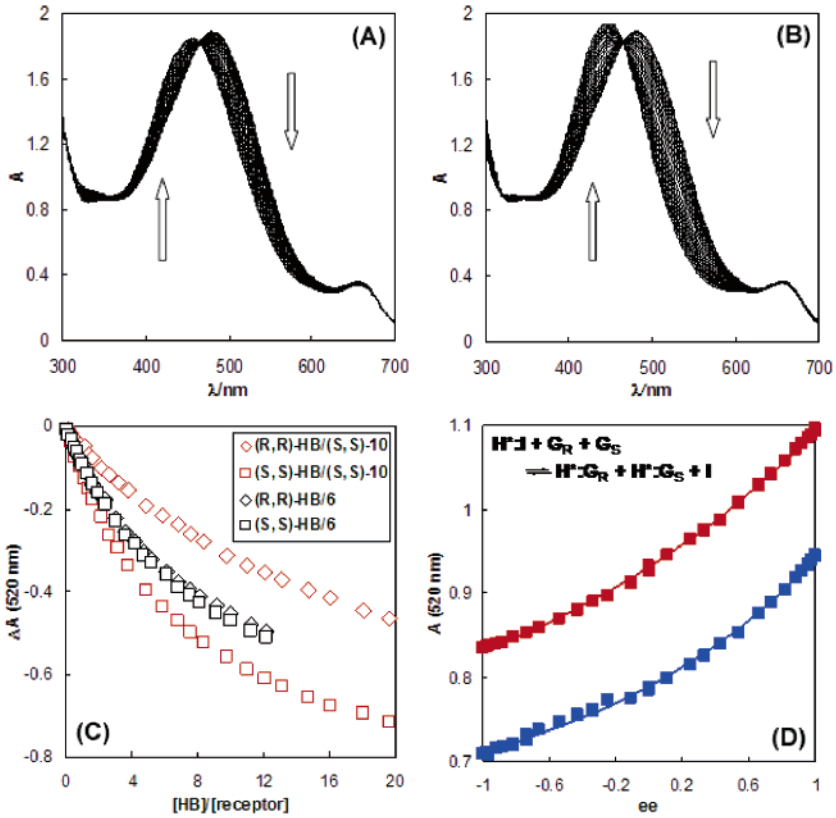

Figure 6. (A) Absorption spectra of PV (149 μM) and (*S*,*S*)-**10** (0.51 mM) in the default buffer (footnote, Figure 3) in the presence of 0−10 mM of (*R*,*R*)-HB. (B) Absorption spectra of PV (149 μM) and (*S*,*S*)-**10** (0.51 mM) in the default buffer in the presence of 0−10 mM of (*S*,*S*)-HB. (C) Absorbance change at 520 nm of PV (149 μM) and receptor (*S*,*S*)-**10** (0.51 mM) or **6** (0.82 mM) in the default buffer with increasing concentrations of (*R*,*R*)- or (*S*,*S*)-HB. (D) Absorbance at 520 nm of PV (149 μM), (*S*,*S*)-**10** (0.51 mM), and HB solutions upon increasing ee of (*R*,*R*)-HB. Blue, $[G]_t = 15$ mM; red, $[G]_t = 7.5$ mM. Solid lines are theoretical curves generated from iterative data fitting. The association constants extracted from the fittings are (the average from two total concentrations): $K_R = 387 \pm 15$ M^{-1}; $K_S = 1136 \pm 78$ M^{-1}.

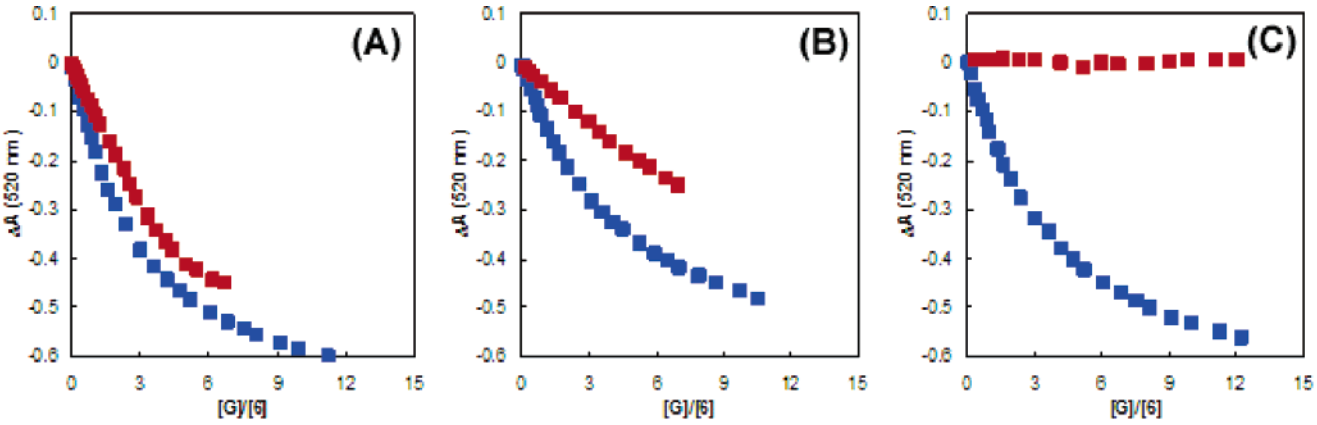

Figure 7. (A) Absorbance change at 520 nm of PV (149 μM) and receptor **6** (0.82 mM) in the default buffer (footnote, Figure 3) with increasing concentrations of L-PL (blue) and PP (red); $K_{PP} \approx 1.2 \times 10^3$ M^{-1}. (B) Absorbance change at 520 nm of PV (149 μM) and receptor **6** (0.82 mM) in the default buffer with increasing concentrations of L-LC (blue) and PVA (red); $K_{LC} = 1.0 \times 10^3$ M^{-1}, $K_{PVA} \approx 300$ M^{-1}. (C) Absorbance change at 520 nm of PV (149 μM) and receptor **6** (0.82 mM) in the default buffer with increasing concentrations of *S*-MD (blue) and BF (red). The association constants between pyruvic acids (PP and PVA) and **6** were estimated with the competitive spectrophotometric method, because their binding behaviors are also subject to processes other than solution equilibria.

75−85% indicator saturation in the absence of analytes was best.

As an example, these empirical criteria were applied in the enantioselective binding studies between (*S*,*S*)-**10** and HB. PV was again chosen as the indicator because of its weaker affinity, which was relatively close to that between HB and (*S*,*S*)-**10**. $[I]_t$ was set at 140 μM where the absorbance at 520 nm (the analyzed wavelength) was 1.7 when PV was saturated by the receptor (*S*,*S*)-**10**. In the displacement assays, an $[H]_t$ concentration (0.51 mM) was chosen to saturate the indicator at an 80% level at the inception. The absorbance at 520 nm decreased to different extents upon titration of the two enantiomers (Figure 6A, B). When the total analyte concentration ($[G]_t$) ranged from 4 to 15 mM, the chiral resolution of the enantioselective assay ($\Delta A = |A_R - A_S|$) was almost constant at 0.25 (Figure 6C). Therefore, this assay was optimized for an ee determination

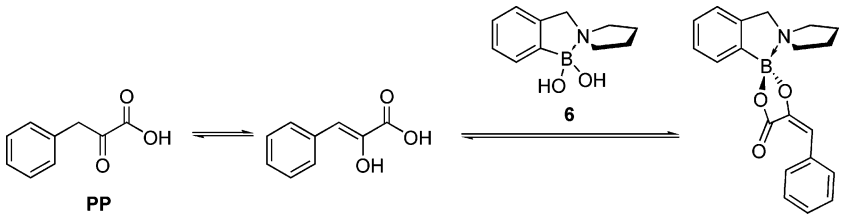

Figure 8. Keto−enol tautomerization of phenyl pyruvic acid (PP) leads to its association with boronic receptors such as **6**.

Table 6. Determination of ee's of 7 HB Samples by Spectrophotometry

sample no.	1	2	3	4
actual ee ($[G]_t = 7.5$ mM)	0.92	0	−0.98	
determined ee	0.85	−0.09	−1.09	
actual ee ($[G]_t = 15$ mM)	0.96	0.82	0	−0.82
determined ee	1.02	0.88	0.13	−0.59

when an HB sample's total concentration was within 4−15 mM. The absorbance (A) vs ee correlation is shown in Figure 6D at two different concentrations ($[G]_t$). When $[G]_t = 7.5$ mM, the red curve shows that the absorbance at 520 nm, where the bound indicator (H:I) absorbs, increases with the growing ee of (*R*,*R*)-HB (ee_R), the weaker binding enantiomer. The absorbance change as a function of ee (dA/dee_R) increases as the ee_R is getting larger (Figure 6D). This is because the assay is more responsive to the change of stronger binding enantiomer concentration ($\Delta[G]_S$) when its concentration ($[G]_S$) is relatively small than otherwise. When $[G]_t$ is increased to 15 mM, the overall absorption profile (blue) is ∼0.12 absorbance units lower due to more competitive binding, while the other features remain. The assay responds to the change of $[G]_t$ and ee similarly to what was observed in the fluorescence studies, indicating that the assay's behavior reliably follows the laws governing solution multiequilibria.

Seven data points were randomly selected from the two ee curves (Figure 6D) as unknown samples. As described above, the curves were fit with the remaining data to determine values of K_R and K_S. The ee values of the seven designated unknown HB samples were determined (Table 6) using a protocol similar to that with fluorimetry described in the previous section. The errors were within 10% of the actual values, except for the one datum point that was at the least sensitive end of the ee curve. Similar failure at such data region was also observed in the fluorescence assay. The nonlinear ee vs A response originates from the different association of two enantiomeric compounds with one chiral receptor. In a future development, the enantiomeric receptor may need to be incorporated into the assay to compensate for the accuracy at the low sensitivity end of the ee curve.

The affinities between three substituted pyruvates were also studied with indicator-displacement assays, because they are the synthetic precursors of α-hydroxycarboxylates through hydrogenation. Quite unexpectedly, substituted pyruvates bearing β-proton(s) bound with boronic acid receptors such as **6** with various strengths. Apparently the enol form of substituted pyruvates led to the formation of complexes (Figure 8). As shown in Figure 7A, PP and PL have comparable affinities to **6**. The tautomerization of the keto form of PP affords an enolate structure that is stabilized through conjugation with the neighboring phenyl ring (Figure 8), which leads to a strong association with receptor **6**. Pyruvic acid (PVA), which lacks the extra stabilization for its enol form, displays less, albeit significant affinity to receptor **6** (Figure 7B). Benzoyl formic acid (BF), which does not have β-protons and therefore is not able to tautomerize, does not associate with **6** (Figure 7C).

Conclusion

In our continuing endeavor to develop assays for analyzing chiral samples with unknown concentrations and enantiomeric excesses, enantioselective indicator-displacement assays were created for α-hydroxycarboxylates and vicinal diols. The chemical basis for the assays is the enantioselective, reversible covalent associations between chiral boronic acid receptors and chiral analytes. Several indicators, colorimetric or fluorescent, constituted the reporting module of the assays and were found to act as secondary tuning units for the enantioselectivity (chiral resolution) and sensitivity of the assays. Specifically, fluorescent indicator 4-methylesculetin (ML) and colorimetric indicators pyrocatechol violet (PV) and alizarin complexone (AC) provided a broad dynamic range where the enantioselective indicator-displacement assays are effective in analyzing chiral α-hydroxyacid and diol samples.

Furthermore, facing the difficulty in determination of both the concentration and the ee of a chiral sample, a mathematical analysis was applied to the displacement system to enable the rapid concurrent determinations of the aforementioned two parameters. An iterative curve fitting program was created that enabled the determination of association constants between a chiral receptor and its enantiomeric substrates by iterative fitting of absorbance (or fluorescence intensity) vs ee curves with the commercial software Origin. Among the association constants between receptors and analytes determined from three different approaches: traditional competitive binding method, iterative fitting of competitive binding curves with enantiomeric pure analytes, and iterative fitting of A (or F) vs ee curves at fixed total concentrations, respectively; the values from the last approach were found to be best suited for the unknown chiral sample analysis. As a result, the accuracy in ee measurements was improved with the optimized protocols.

Acknowledgment. We thank NIH (GM65515) for financial support.

Supporting Information Available: Syntheses, titration procedures, and mathematical analysis of competitive binding processes (PDF). This material is available free of charge via the Internet at http://pubs.acs.org.

JA0435945